

Neutralisation rate controls the self-assembly of pH-sensitive surfactants

Dominic W. Hayward^{*a,b}, Leonardo Chiappisi^{a,b}, Jyh Heng Teo^b, Sylvain Prévost^b, Ralf Schweins^b, and Michael Gradzielski^{*a}

^aStranski-Laboratorium für Physikalische und Theoretische Chemie, Institut für Chemie, Technische Universität Berlin, Straße des 17. Juni 124, D-10623 Berlin, Germany

^bInstitut Laue-Langevin, 71 avenue des Martyrs, CS 20156, 38042 Grenoble cedex 9, France

*hayward@ill.fr, michael.gradzielski@tu-berlin.de

S1 Further Details Relating to the SANS Analysis

S1.1 Rebinning

In order to simplify the fitting procedure, the data taken from the three instrument configurations were combined into one dataset and rebinned to reduce the number of data points. This was done in three steps:

1. The entire Q -range is split up into N bins distributed evenly in $\log(Q)$
2. Each data point is assigned to its corresponding bin
3. The average intensity and uncertainty is calculated for each bin

Table S1. Summary of the densities, neutron scattering length densities and volumes used in the scattering model.

	Density (g/cm ³)	Neutron SLD (10 ⁻⁶ Å ⁻²)	Volume (Å ³)
D ₂ O	1.11	6.39	30
Hydrophobic segment	0.75	-0.31	340
Hydrophilic segment	1.25	1.33	341

S2 Further Details Relating to the DLS Analysis

S2.1 Calculation of the Weight Fractions

To estimate the weight fraction of vesicles in the surfactant solutions, the first-order field correlation functions from the dynamic light scattering data were first fitted to a bimodal exponential model of the form:

$$g^{(1)}(\tau, Q) = A \cdot \exp(-D_1 Q^2 \tau) + (1 - A) \cdot \exp(-D_2 Q^2 \tau) \quad (\text{S1})$$

where A and $(1 - A)$ are the relative intensity contributions from components 1 and 2 respectively. The weight fractions of each component were then be obtained by taking into account the respective volumes of the scatterers following the method of Shibayama *et. al.*¹ modified to take into account the scattering from a mixture of micelles and vesicles:

$$w_m = \begin{cases} \frac{A/V_m}{A/V_m + (1-A)/V_v} & QR_m < 1.78 \text{ and } QR_v < 1.1 \\ \frac{A/V_m}{A/V_m + ((1-A)/V_v) \cdot (QR_v)^2/1.1^2} & QR_m < 1.78 \text{ and } QR_v \geq 1.1 \\ \frac{(AR_m Q^4)/1.78^4}{(AR_m Q^4)/1.78^4 + ((1-A)/V_v) \cdot (QR_v)^2/1.1^2} & QR_m \geq 1.78 \text{ and } QR_v \geq 1.1 \end{cases} \quad (\text{S2})$$

where w_m is the weight fraction of the micelle fraction, V_m and R_m are the volume and radius of the micelles, V_v and R_v are the volume and radius of the vesicles and Q is the scattering vector. Briefly, the significance of the value $QR_m \sim 1.78$ arises from the crossover point where the form factor of the scattering from a spherical particle changes from a plateau (at low- Q) to a Porod function (at high- Q), hence the Q^{-4} dependence. Similarly, the value $QR_v \sim 1.1$ arises from the crossover point where the form factor of the scattering from a locally flat particle, changes from a plateau to a Q^{-2} dependence.

S3 Supplementary Table

Table S2. Tabulated mean aggregation numbers as calculated from the plateau of the corresponding static light scattering data (shown in Figure S6). Data are shown graphically in Figure 4b in the main text.

NaOH Addition Rate (eq./s)	Base Concentration (mol/L)	Mean Aggregation Number
2.78×10^{-3}	0.1	49
3.70×10^{-4}	0.1	56
3.70×10^{-5}	0.1	52
3.70×10^{-6}	0.1	92
3.70×10^{-7}	0.1	442
3.70×10^{-8}	0.1	3653
2.78×10^{-3}	1	46
3.70×10^{-4}	1	63
3.70×10^{-5}	1	60
3.70×10^{-6}	1	167
3.70×10^{-7}	1	419
3.70×10^{-8}	1	2615
2.78×10^{-3}	10	62
3.70×10^{-4}	10	68
3.70×10^{-5}	10	68
3.70×10^{-6}	10	99

S4 Supplementary Figures

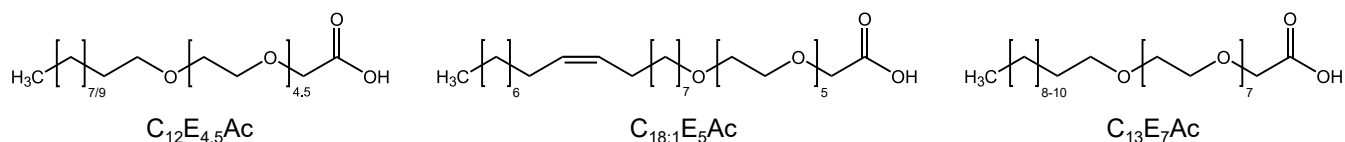


Figure S1. Approximate chemical structures of the three principal surfactants used in this work. Note that the materials are technical surfactants and therefore have a significant associated polydispersity, as can be seen in Figure S2.

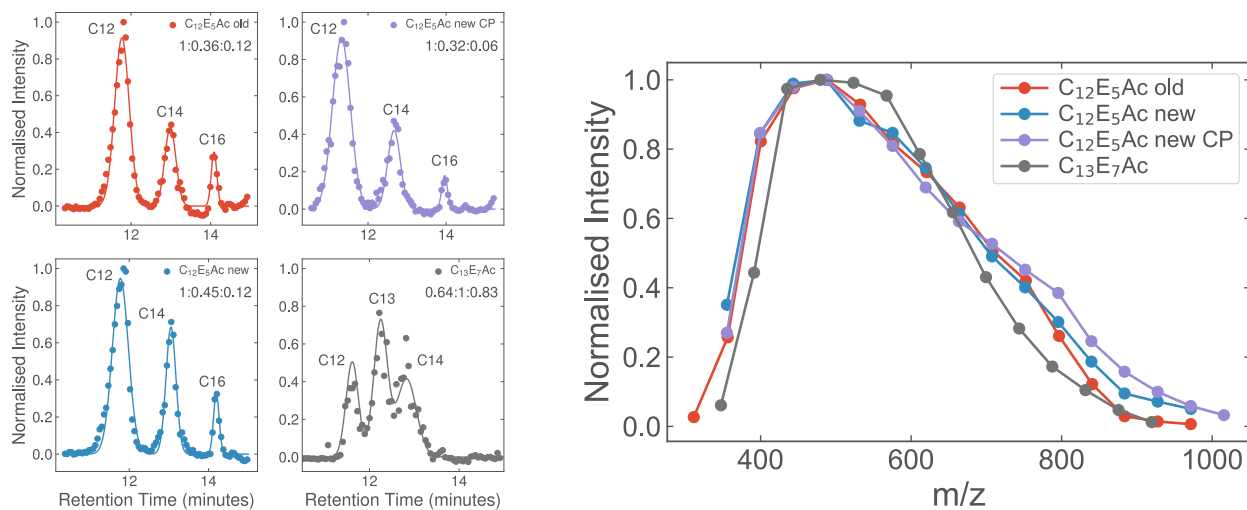


Figure S2. Electrospray ionisation mass spectra of the C₁₂E₅Ac materials used in this study. The spectra of C₁₃E₇Ac are also shown for comparison. Figures on the left show the chromatograms with the relative proportions of C12:C14:C16 (C12:C13:C14 for C₁₃E₇Ac) chains found in the surfactants. The figure on the right shows the mass spectrum for the C12 peak (C13 for C₁₃E₇Ac).

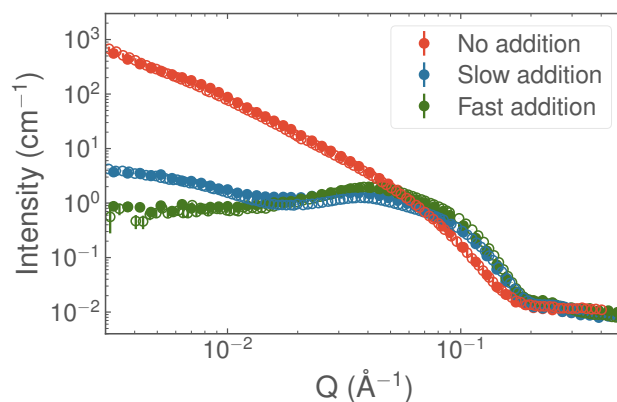


Figure S3. Azimuthally averaged SANS data from 1 %wt solutions of C₁₂E₅Ac, showing both the original batch (closed symbols) and the batch used in this study (open symbols). In all cases the ‘slow’ addition speed was 3.7×10^{-6} eq. s⁻¹ and the fast addition speed was 2.8×10^{-3} eq. s⁻¹.

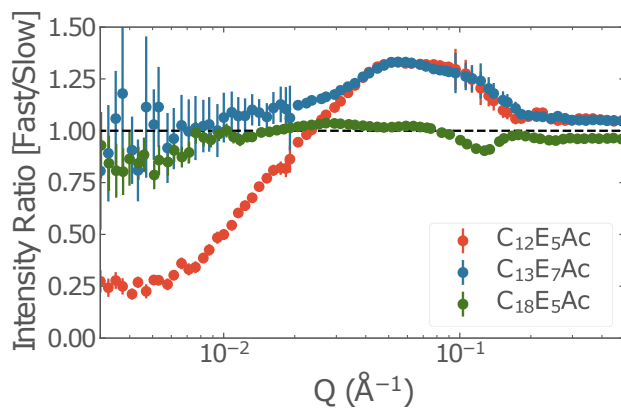


Figure S4. Ratio of the azimuthally averaged SANS data from the fast and slow additions of 1 M NaOH to 1 %wt solutions of $C_{12}E_5Ac$. The ‘slow’ addition speeds were 3.7×10^{-6} , 4.5×10^{-6} and 4.7×10^{-6} eq. s^{-1} and the fast addition speeds were 2.8×10^{-3} , 3.4×10^{-3} and 3.6×10^{-3} eq. s^{-1} for the $C_{12}E_5Ac$, $C_{13}E_7Ac$ and $C_{18:1}E_5Ac$ samples respectively

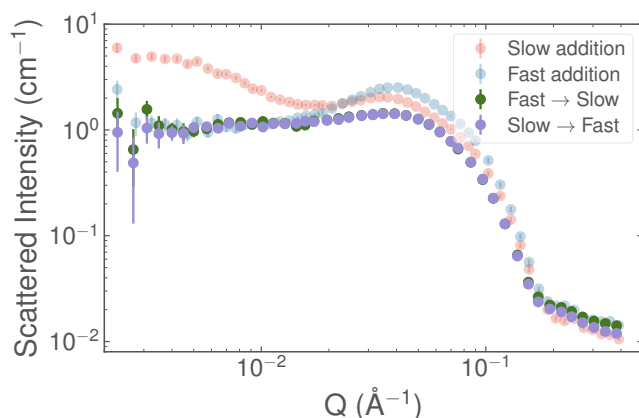


Figure S5. Azimuthally averaged SANS data from 1 %wt solutions of $C_{12}E_5Ac$, showing both the original batch (closed symbols) and the batch used in this study (open symbols). In all cases the ‘slow’ addition speed was 3.7×10^{-6} eq. s^{-1} and the fast addition speed was 2.8×10^{-3} eq. s^{-1} .

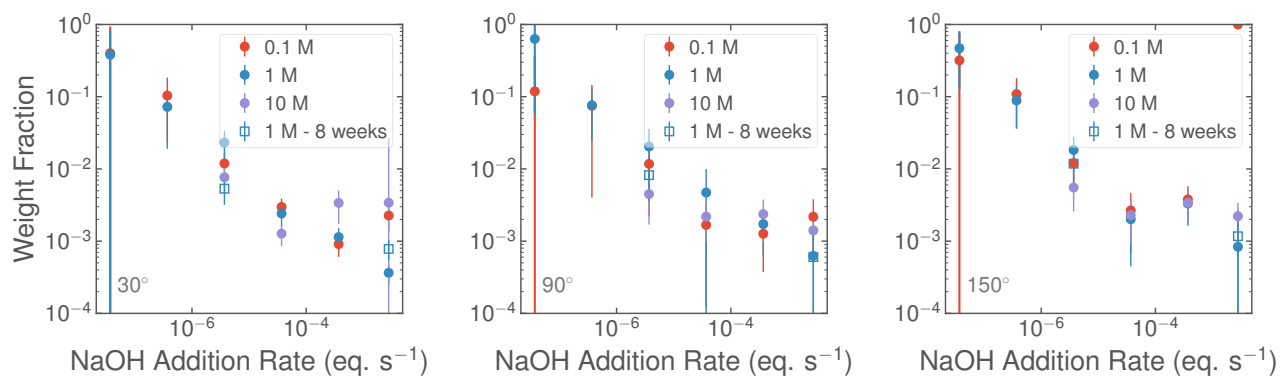


Figure S6. Weight fractions of surfactant in vesicle form in 1 wt% solutions of $C_{12}E_5Ac$ after the addition of NaOH at various concentrations and addition rates. Plots show results taken at 30° , 90° and 150° . A plot showing the average of all measurements in the range 30° – 150° is given in Fig 4a in the main text.

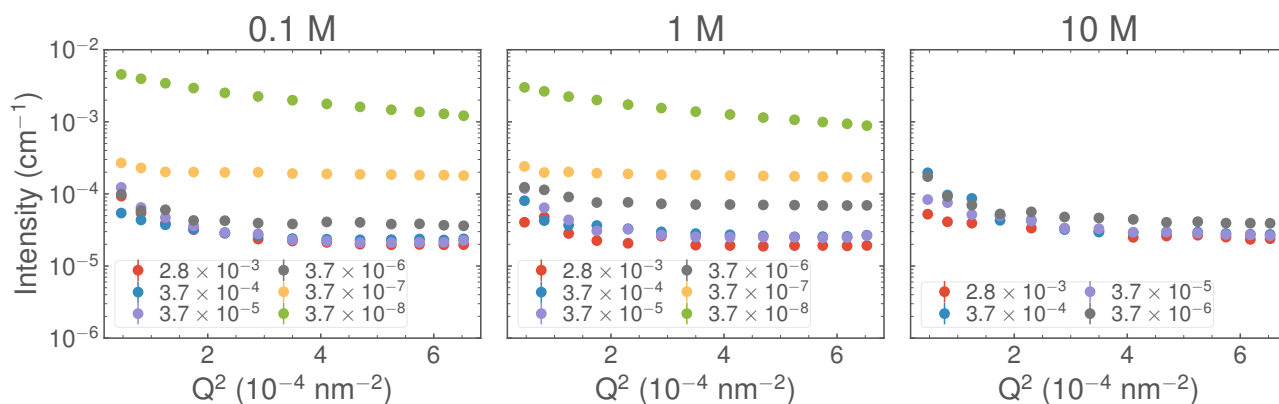


Figure S7. Static light scattering data collected at pH 10 following that addition of NaOH to $C_{12}E_5Ac$. The plot subtitles indicate the concentration of the NaOH and the plot legends indicate the addition speeds in eq/s.

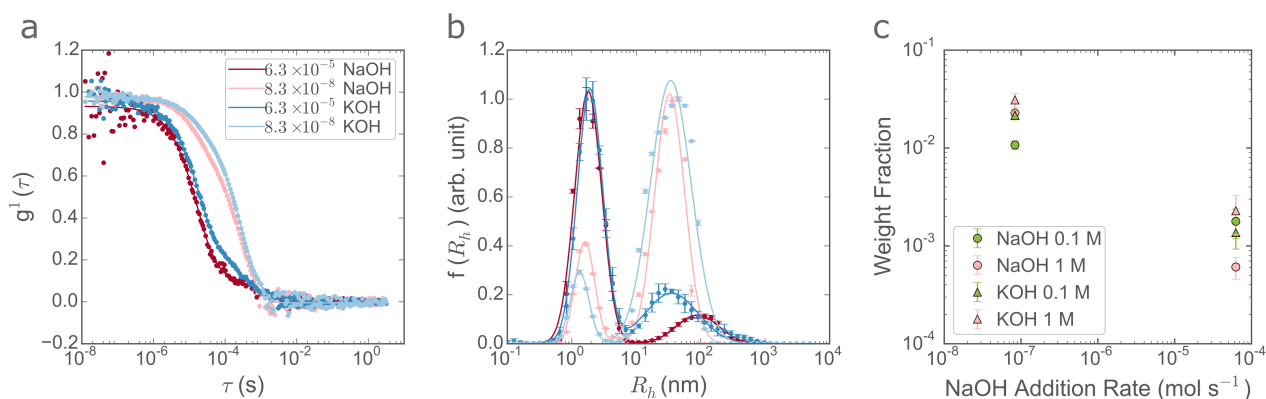


Figure S8. DLS correlation functions (a), the corresponding size distribution functions (b) and the related weight fraction of vesicles (c) from 1 wt% solutions of $C_{12}E_5Ac$ after the addition of 1 M NaOH and 1 M KOH.

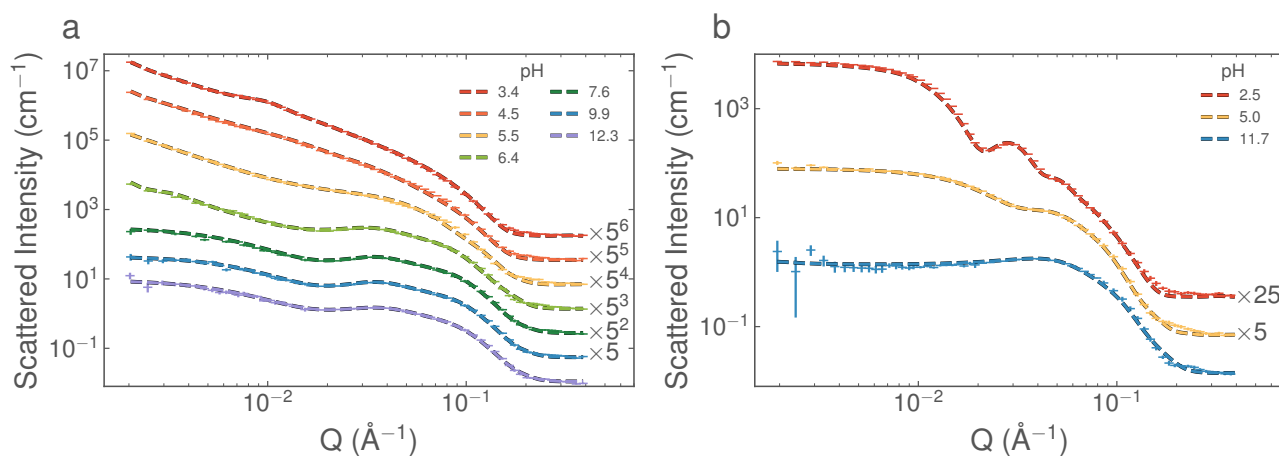


Figure S9. Azimuthally averaged SANS data from 1 %wt solutions of $C_{12}E_5Ac$, previously published in reference² showing the structural changes occurring as the pH is increased via the slow addition of NaOH (a) and the corresponding slow addition of NaOH in the presence of 24.5 mM NaOH (b).

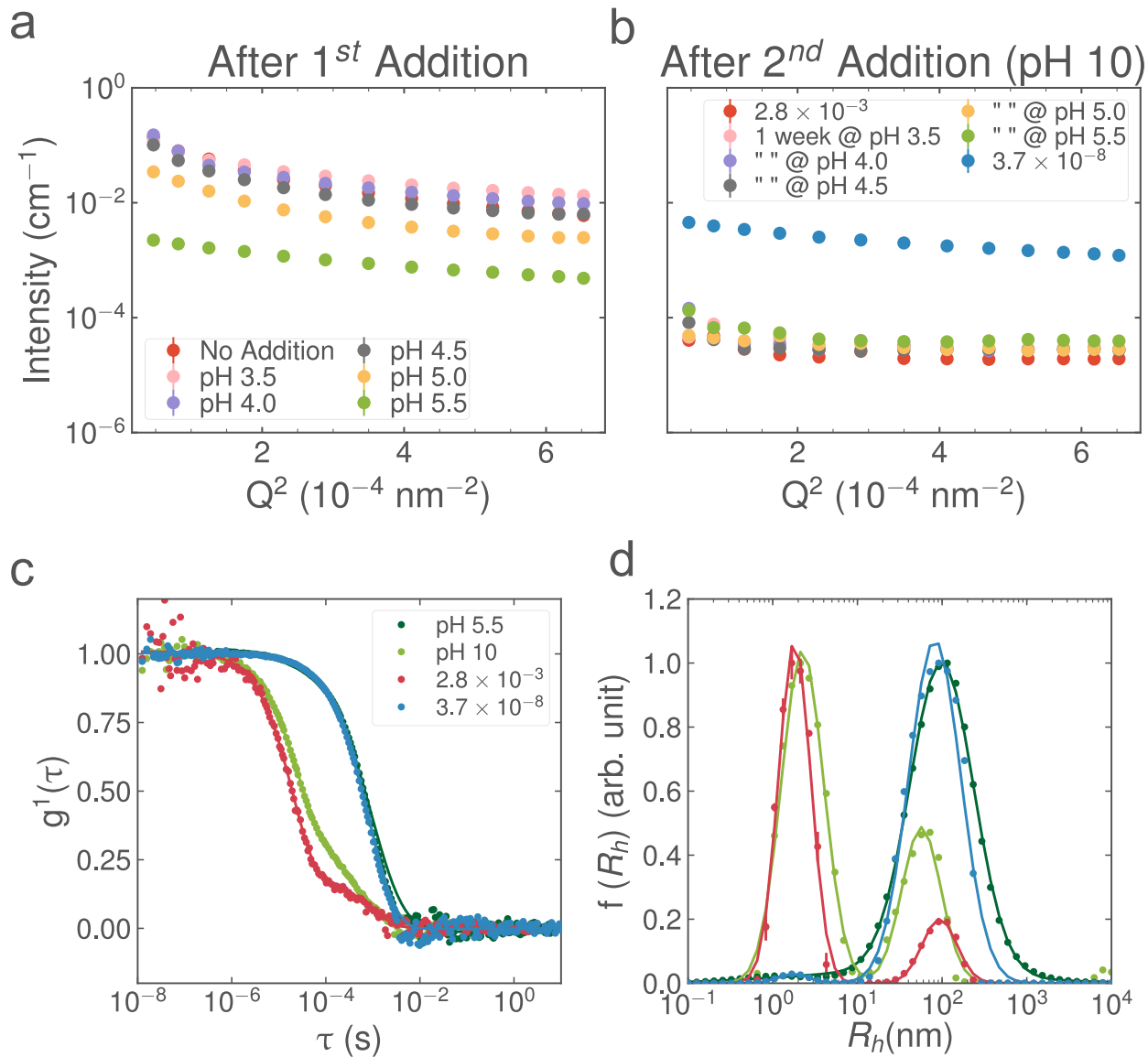


Figure S10. (a) Static light scattering data collected after an initial fast addition of NaOH to $C_{12}E_5Ac$ to achieve the desired pH. (b) Static light scattering data collected from the same samples after a period of 7 days at the indicated pH followed by a second rapid addition of NaOH to bring the samples up to pH 10. Plot (c) shows the DLS correlation functions and (d) the corresponding size distribution functions of the sample maintained at pH 5.5 before and after the second addition of NaOH. In plots (b-d), data from the continuous additions at $2.8 \times 10^{-3} eq. s^{-1}$ and $3.7 \times 10^{-8} eq. s^{-1}$ are shown for comparison.

References

1. M. Shibayama, T. Karino and S. Okabe, *Polymer*, 2006, **47**, 6446–6456.
2. D. W. Hayward, L. Chiappisi, S. Prévost, R. Schweins and M. Gradzielski, *Sci. Rep.*, 2018, **8**, 7299.